ARL-TR-7581 ● JAN 2016

US Army Research Laboratory

Stabilization of Gold Nanorods (GNRs) in Aqueous and Organic Environments by Select Surface Functionalization

by Devon A Boyne, Alin C Chipara, Lily Giri, and Mark H Griep

NOTICES

Disclaimers

The findings in this report are not to be construed as an official Department of the Army position unless so designated by other authorized documents.

Citation of manufacturer's or trade names does not constitute an official endorsement or approval of the use thereof.

Destroy this report when it is no longer needed. Do not return it to the originator.

ARL-TR-7581 ● JAN 2016

US Army Research Laboratory

Stabilization of Gold Nanorods (GNRs) in Aqueous and Organic Environments by Select Surface Functionalization

by Devon A Boyne and Lily Giri
Oak Ridge Institute for Science and Education, Oak Ridge, TN

Alin C Chipara
College Qualified Leaders (CQL) Program, ASEE

Mark H Griep
Weapons and Materials Research Directorate, ARL

REPORT DOCUMENTATION PAGE

Form Approved
OMB No. 0704-0188

1. REPORT DATE *(DD-MM-YYYY)*	2. REPORT TYPE	3. DATES COVERED (From - To)
January 2016	Final	May 2015–July 2015

4. TITLE AND SUBTITLE
Stabilization of Gold Nanorods (GNRs) in Aqueous and Organic Environments by Select Surface Functionalization

5a. CONTRACT NUMBER

5b. GRANT NUMBER

5c. PROGRAM ELEMENT NUMBER

6. AUTHOR(S)
Devon A Boyne, Alin C Chipara, Lily Giri, and Mark H Griep

5d. PROJECT NUMBER

5e. TASK NUMBER

5f. WORK UNIT NUMBER

7. PERFORMING ORGANIZATION NAME(S) AND ADDRESS(ES)
US Army Research Laboratory
ATTN: RDRL-WMM-A
Aberdeen Proving Ground, MD 21005-5069

8. PERFORMING ORGANIZATION REPORT NUMBER
ARL-TR-7581

9. SPONSORING/MONITORING AGENCY NAME(S) AND ADDRESS(ES)

10. SPONSOR/MONITOR'S ACRONYM(S)

11. SPONSOR/MONITOR'S REPORT NUMBER(S)

12. DISTRIBUTION/AVAILABILITY STATEMENT
Approved for public release; distribution is unlimited.

13. SUPPLEMENTARY NOTES

14. ABSTRACT
The stability of gold nanorods (GNRs) is essential for their integration into functional materials. In this work, the stability of GNRs in organic and aqueous solvents is improved by using various stabilizing layers. The retention of the optical properties of the GNRs is confirmed by ultraviolet-visible and zeta-potential measurements. Additionally, 3 different methods are applied to achieve self-assembly of GNRs onto copper grids. Ultimately, these studies demonstrate the versatility and stability of GNRs with regard to their use in integrated functional systems.

15. SUBJECT TERMS
nanoplasmonics, gold nanorods, solution stability, self-assembly, surface functionalization

16. SECURITY CLASSIFICATION OF:			17. LIMITATION OF ABSTRACT	18. NUMBER OF PAGES	19a. NAME OF RESPONSIBLE PERSON
a. REPORT	b. ABSTRACT	c. THIS PAGE			Mark Griep
Unclassified	Unclassified	Unclassified	UU	26	19b. TELEPHONE NUMBER (Include area code) 410-306-4953

Contents

List of Figures

List of Tables

Acknowledgments

The authors would like to thank Abby West and Alexis Fakner for their assistance in material synthesis and Scott Walck for instruction on the transmission electron microscope. Alin Chipara would like to acknowledge the American Society for Engineering Education College Qualified Leaders program for sponsorship, and Devon Boyne would like to thank the Oak Ridge Institute for Science and Education (ORISE) for support through a postdoctoral fellowship.

This research was supported in part by an appointment to the Postgraduate Research Participation Program at the US Army Research Laboratory (ARL) administered by ORISE through an interagency agreement between the US Department of Energy and ARL.

INTENTIONALLY LEFT BLANK.

1. Introduction and Background

Gold nanorods (GNRs) are a unique nanomaterial that exhibit tunable plasmonic properties based on the nanorod's aspect ratio. The ability to tune GNR interaction with electromagnetic (EM) radiation as a function of GNR size and aspect ratio has been harnessed in multiple research areas including biomedical engineering,[1–3] optoelectronics,[4] and photovoltaics.[5,6] The optical properties of these metallic nanomaterials are based on a phenomenon known as localized surface plasmon resonance (LSPR) in which photons couple with plasmons (collective oscillations of electrons about a metallic nanoparticle) and display a strong absorption in an optical transmission spectra (Fig. 1). The wavelength (λ_{LSPR}) at which this absorption occurs is extremely sensitive to changes in the material dimensions, surface functional groups, and the local environment (i.e., dielectric changes) representing the basis of sensing studies.[7]

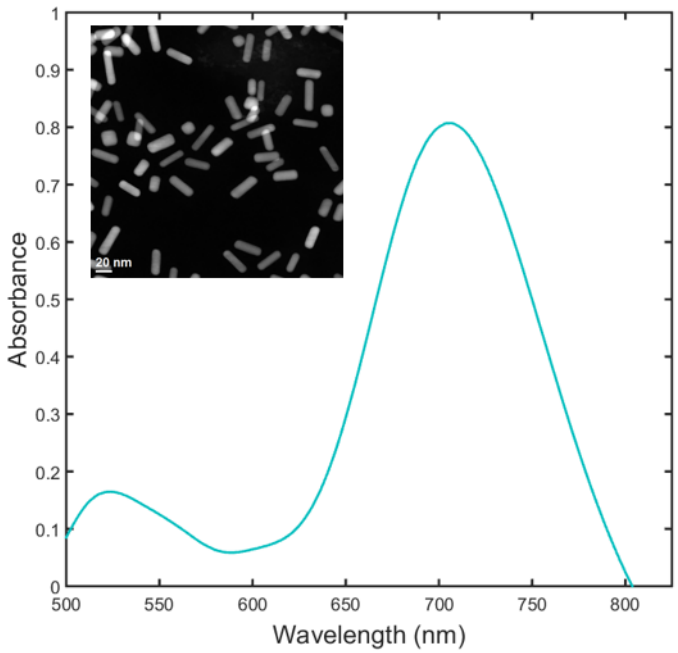

Fig. 1 Spectra for a typical absorption spectra for GNRs; inset: dark-field scanning transmission electron microscope (TEM) image of GNRs

For many applications, GNRs need to be integrated into a functional composite system without experiencing aggregation or other degradation mechanisms; knowledge of the stability of GNRs in a wide array of solvents is therefore essential to enable solution processing of cast thin-film composites. However, the traditional methods for synthesizing GNRs result in materials that are stabilized by micelles incompatible with, and unstable in the presence of, many solvents and potentially

both biological species and polymers.[8] In organic solvents, aggregation can diminish the GNRs' optical properties.[9] To reduce the driving force for aggregation, the micellar structure must be protected or replaced by functional groups that increase GNRs' solvent stability.[9] In this work, GNRs were functionalized with polyelectrolyte monolayers (PEMs), polyethylene glycol (PEG), and silica (Si) shells in an effort to broaden the accessible solvent range for increased compatibility in composite materials. Surface functionalization of the GNRs was suggested by changes in surface charge and LSPR wavelength ($\Delta\lambda_{LSPR}$). The stability in various solvents was monitored by observing the $\Delta\lambda_{LSPR}$, which exhibited a linear shift toward higher wavelengths (red shift) with increasing solvent refractive index (RI). Furthermore, the self-assembly of GNRs was investigated by 3 different methods to obtain nonaggregated GNRs that retained their plasmonic properties.

2. Materials and Methods

Unless specified, all chemicals were purchased from Sigma-Aldrich (St. Louis, MO) and made in aqueous solutions. Stock solutions of 0.2-M cetyl trimethyl ammonium bromide (CTAB) were prepared and kept at 29 °C (below 29 °C 0.1-M CTAB will crystalize); aliquots were diluted appropriately throughout the synthesis procedure. Similarly, a stock solution of 0.02-M sodium salicylate (Na-Sal) in 0.1-M CTAB was prepared and stored at 29 °C (dissolution of Na-Sal obtained by sonication under heating for approximately 1–2 h). A large batch of 50-mM chloroauric acid was kept at 4 °C for up to 1 month (the solution was brought to room temperature prior to use). Stock solutions of silver nitrate ($AgNO_3$) were kept at 4 °C and discarded after 4 days. Finally, 0.1-M hydroquinone (HQ) was made in large batches and maintained in solution at 4 °C for up to 2 weeks; after 2 weeks, old solutions often became a yellowish color.

2.1 Synthesis of Gold (Au) Nanoseed Solution

The synthesis of Au nanoseeds is described in detail elsewhere.[10,11] Briefly, 100 μL of 50 mM and 990 μL of 0.1-M CTAB were prepared. Added to this solution under rapid stirring was 0.46 mL of ice cold 0.1-M $NaBH_4$ (sodium borohydride) in 0.01-M sodium hydroxide (NaOH). The addition of the reducing agent caused an abrupt color change from orange to dark grey with a red tint. Trials using seed solutions with a different shade of color (suggesting a different concentration) did not produce significantly different results ($\Delta\lambda_{LSPR}$ ~725 <10 nm).

2.2 Nanorod Growth

The procedure for preparing growth solutions was modified from Zubarev et al.[12] to incorporate a weaker reducing agent than typically used for seed-mediated growth. If the ratio of reactants is maintained, the procedure can be scaled up or down to a desired volume; the method described herein is for a 10-mL total volume. Initially, 100 uL of 0.004-M $AgNO_3$ (4×10^{-7} mole) was added to 5 mL of 0.02-M Na-Sal (1×10^{-4} mole, 250 equivalent). The solution was gently mixed and then incubated at 29 °C for 15–30 min. Following the incubation period, 5 mL of 1-mM $HAuCl_4$ (5×10^{-6} mole) was added to the growth solution. This solution was shaken for 15 min at room temperature, during which the solution changed from pale gold to clear, signifying partial reduction of Au(III) to Au(I).[13] To complete the reduction [Au(I) to Au(0)], 250 μL of 0.1-M HQ (2.5×10^{-5} mole) was added and the solution was shaken gently for 30 s to 1 min. Finally, 0.16 uL of the seed solution was added, gently shaken approximately 15 s, and left undisturbed overnight at 29 °C.

2.3 Purification of Growth Solutions

Following the growth stage, the GNRs were purified by centrifugation at 10,000 rpm for approximately 30–45 min. The supernatant was then removed and the rods were redispersed in either water or 0.01-M CTAB, with the latter primarily used for longer-term material storage. Prior to functionalization, the GNRs were isolated by centrifugation and redispersed in water twice to minimize excess CTAB in solution.

2.4 Surface Functionalization

Purified GNRs were functionalized with polyelectrolyte layers and polyethylene glycol thiol (PEG-SH) by methods previously described in Alkinlany et al.[9] and Pierrat et al.,[14] respectively. For PEM functionalization, layer-by-layer deposition was applied beginning with the negatively charged species [poly(vinylsulfonic acid) (PVSA)] or polystyrene sulfonate (PSS) followed by the positively charged species [poly(allyamine hydrochloride) (PAH)]. The initial charge of the GNR was positive due to a base layer of CTAB. Briefly, 1 mL of 0.1-M NaCl was added to 10 mL of the purified GNR and briefly vortexed, then 1 mL of freshly prepared 0.1-mM PEM was added, vortexed, and incubated while shaking at room temperature for a minimum of 30 min. The pH of the solution was not adjusted prior to functionalization; pH = 6.85 (PSS) and 3.55 (PAH). To remove unreacted PEMs, the solutions were centrifuged for 30–45 min at 10,000 rpm. The procedure was repeated for subsequent layers.

For PEG-SH functionalization, 1 mL of 2-mM PEG-SH (2 moles) was added to 9 mL of GNR. The solution was briefly vortexed and incubated while shaking at room temperature for 1.5 h. The PEG-SH displaces the CTAB and binds directly to the GNR. All water used for this procedure was degassed (including the last GNR purification). Unreacted species were removed via centrifugation.

Si-capped GNRs were prepared by a method described by Murphy et al.[15] The final concentration of CTAB in solution was adjusted to 0.7 mM prior to Si growth. The following procedure is for 10 mL of solution, though it could be scaled to larger volumes. Initially, the pH of the CTAB-GNR solution was adjusted to approximately 10.6 with NaOH (0.1 M) (~40 μL NaOH). The solution was then incubated for approximately 30 min. Finally, 90 μL of dilute tetraethyl orthosilicate (TEOS; 20% in methanol) was injected into the pH-adjusted solution. Following a brief vortexing, the solution was incubated overnight while shaking.

2.5 Solution Stability

The stability of the functionalized GNRs were tested in a variety of solvents with various refractive indices. In general, 1.5 mL of the resultant GNR solution (~1.7-mg/mL GNRs; see Section 2.2) after purification was used for each solvent. Stability was assessed by monitoring $\Delta\lambda_{LSPR}$ and visually observing particle aggregation (i.e., loss of pigmentation and precipitation of agglomerations). If partial dissolution occurred, GNRs were considered unstable in that solvent. Redispersal of the GNRs to the desired solvent required a centrifugation step to pellet out the GNRs and remove the water. The pellets were rinsed 3 times with the respective solvent and brought to a final volume of approximately 100 μL. For solvents with a high hydrophobicity (xylene and chloroform), the GNRs had to be dispersed in acetone as an intermediate step prior to exchange into the desired solvent.

2.6 Self-Assembly: Transmission Electron Microscopy (TEM) Grid Preparation

TEM was used to assess structural properties of GNRs. TEM grids were prepared with PVSA-GNRs, CTAB-GNRs, and PEG-GNRs. For the PVSA-coated GNRs, a fast evaporation method was applied. GNRs were solvent-exchanged into acetone using the procedure described in Section 2.5, then a drop of the solution was deposited onto holey carbon TEM grids (HC300-Cu, Electron Microscopy Sciences, Hatfield, PA), and the acetone was evaporated at room temperature. CTAB-GNRs were prepared in an aqueous phase, and a drop of solution was placed on the TEM grid. The water was allowed to slowly evaporate at room temperature.

Finally, PEG-GNRs were deposited by the Langmuir-Schaefer technique. Briefly, following dispersal in chloroform, 50–100 μL of PEG-GNRs was carefully transferred to a vial (68-mm diameter) containing water. The chloroform was then allowed to evaporate, allowing for self-assembly at the interface of the water and organic phase. TEM grids were then dipped onto the interface and allowed to dry under ambient conditions.

2.7 Instrumental Parameters

The optical properties of the GNRs were determined by ultraviolet-visible (UV-vis) analysis obtained on a Nanodrop 2000 (2 μL of solution, 1-mm path length, Thermo Scientific, Waltham, MA, 180–800 nm). Structural characterization was obtained by TEM on a Jeol 2100 (Jeol, Peabody, MA) at 200 KeV. To determine the surface charge, zeta-potential measurements were taken on a nanoparticle analyzer (HORIBA, Nanopartica SZ-100, Kyoto, Japan).

3. Results and Discussion

3.1 Functionalization and Solution Stability

It is known that CTAB-GNRs exhibit both poor solubility and low stability in water.[9,16–18] To expand the utility of GNRs and enable their use in a wider array of solvent systems, GNRs were functionalized with polyelectrolyte layers (PEMs, polyethylene glycol thiol (PEG-SH,) and Si shells. After functionalization, the GNRs were analyzed using TEM, zeta-potential analysis, UV-vis, and a survey of solubility in an array of solvents of varying polarities.

Zeta potential is an efficient way to measure the electrokinetic potential of colloidal solutions. For charged species, zeta measurements can be used to disseminate the charge of the surface groups. To confirm the successful functionalization of GNRs with PEMs, the zeta potential was monitored (Fig. 2A) with layer numbers of 0,1, and 2, corresponding to exposed surface groups of CTAB (+), PVSA (–), and PAH (+), respectively. Three different batches of GNRs were investigated: nanospheres (λ_{LSPR} = ~520 nm), high aspect-ratio GNRs (λ_{LSPR} = ~750 nm), and low-aspect-ratio GNRs (λ_{LSPR} = ~650). Results obtained for all 3 types follow similar trends (Fig. 2A), which suggests that the morphology of the rod/sphere does not have a significant effect of the assembly of the layers. Therefore, this method may be applied to rods and spheres of different aspect ratios. It is important to mention, however, that for other gold nanoparticle (GNP) geometries (triangles, platelets,

etc.), these results may differ. Additionally, because the PEM is changing the effective refractive index (RI), a $\Delta\lambda_{LSPR}$ is observed (Fig. 2B) for each subsequent layer.

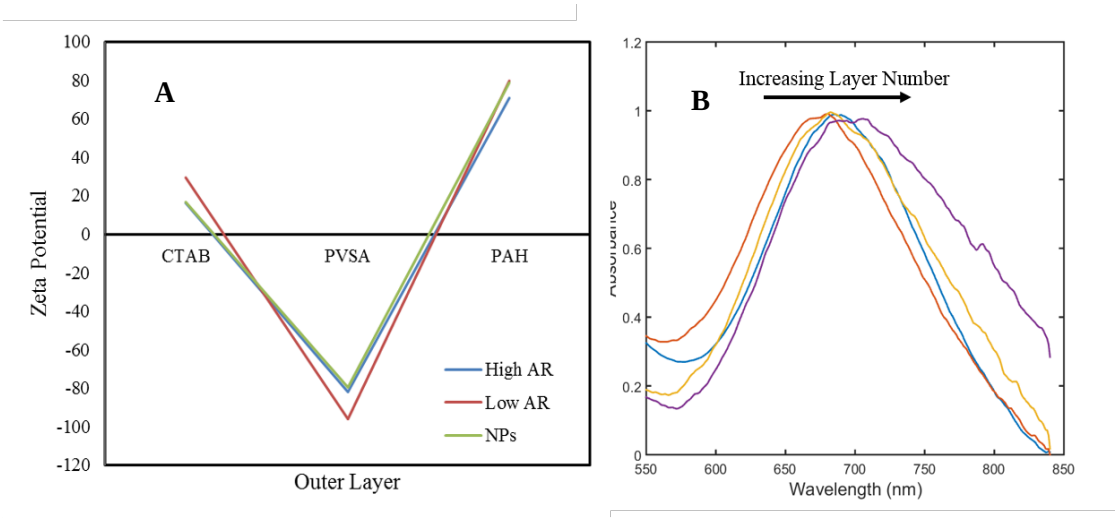

Fig. 2 A) Zeta potential of alternating PEM layers (CTAB: PVSA [–] :PAH [+]) for different shaped nanoparticles and B) red shift of LSPR for alternating PEM layers (no layer: PSS [–]: PAH [+]: PSS [–])

This behavior has been observed previously for planar Au and GNPs by several groups.[9,19] By increasing/decreasing the number of layers, the distance between the GNP and other functional materials can be optimized and lead to enhanced control of the resultant optical properties. Challenges when employing PEM layers to functionalize particles may arise because there is significant loss due to purification of the particles after each functionalization in addition to high sensitivity of λ_{LSPR} to small variations in the thicknesses of the PEMs. Functionalization with different surface groups can also be confirmed by monitoring the λ_{LSPR}. The addition of a surface layer changes the effective refractive index surrounding the particle, causing a shift in the absorption spectrum associated with plasmon resonance. The $\Delta\lambda_{LSPR}$ induced by functionalization with PEG-SH is illustrated in Fig. 3. A blue shift in the optical extinction is observed following exchange of CTAB with PEG-SH. While the peak intensity hardly shifts, the growth of an absorption shoulder indicates new electronic transitions are available to absorb the lower-wavelength light. Interestingly, if only the RI of the surrounding solution were considered, since PEG-SH is a higher refractive index than water (~1.47 refractive index unit [RIU]; Sigma Aldrich), a red shift would be expected. Most likely, this blue shift is representative of a change in the dielectric constant due to the initial binding of the PEG-SH and has been reported to occur for GNRs[9] and planar Au.[20]

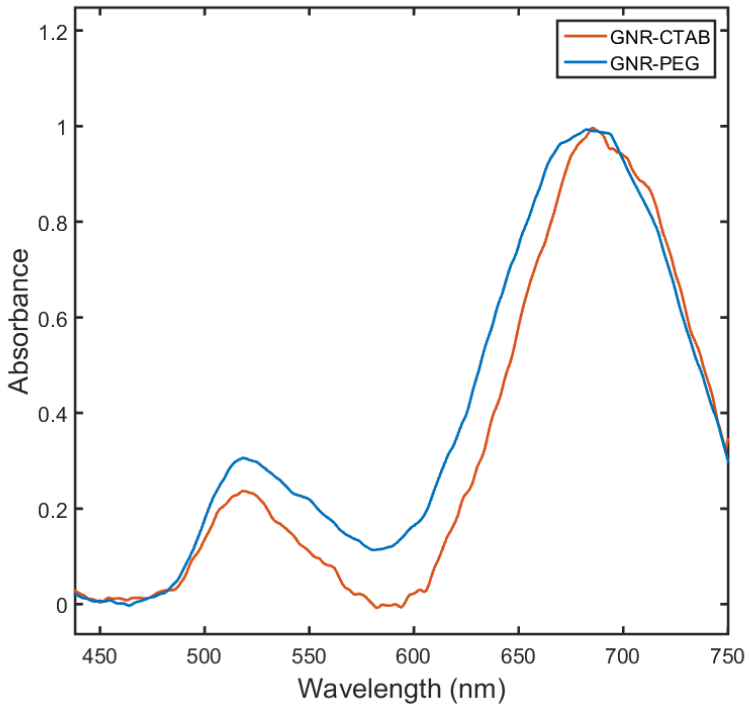

Fig. 3 $\Delta\lambda_{LSPR}$ induced by PEG-SH functionalization for GNRs

Si capping is often applied to improve the temperature stability of GNPs, as electrostatic and thiol bonds can be unstable at temperatures above approximately 100 °C. The increased thermal stability of Si-capped GNRs may expand their utility to composite applications, where processing conditions can require increased cure or annealing temperatures. The loss of aliphatic surfactants around the GNPs meant that their solvent stability/compatibility had to be re-evaluated. Si capping was accomplished by a modified Stober process developed by Murphy et al.[15] and involved the formation and condensation of CTAB/Si particles around the GNR. To confirm the successful functionalization of Si, TEM was performed (Fig. 4). As a result of the differences in electron scattering, a visual contrast was observed between the Au and the Si cap. It is important to note that the thickness of the Si shell can be modified by controlling the concentration of CTAB in solution prior to functionalization. This concentration dependence can effectively be used as a spacer for subsequent functionalization of the Si shell. Lighter blotches are also evident in the TEM and may be indicative of Si nanoparticle formation. The Si nanoparticles may be removed through exhaustive centrifugation and redispersion steps but for the current TEM study they were sufficiently pure to highlight the impacts of Si capping.

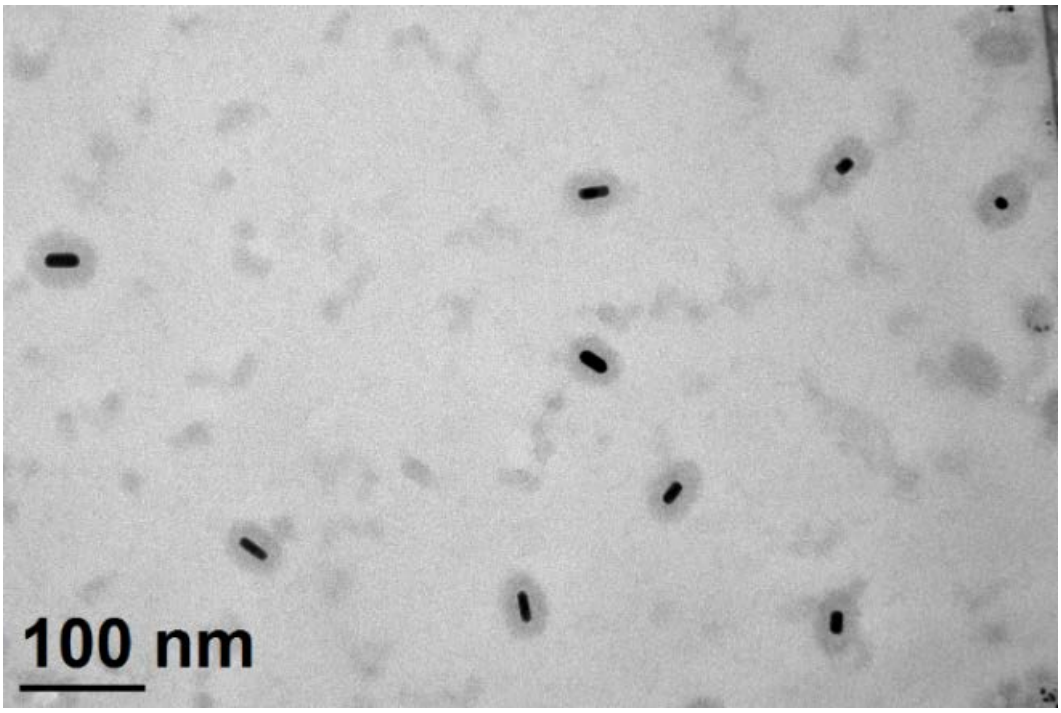

Fig. 4 TEM micrograph of Si-capped GNRs

The temporal solution stability of GNRs was tested in several different solvents and monitored via optical absorption. Unstable species aggregated and displayed no absorption in the optical spectra, spectral broadening, and/or a reduced ratio between the characteristic absorption peaks longitudinal SPR (longer wavelength plasmon occurring along the length of the GNR) and tranverse SPR (shorter wavelength plasmon occurring along the waist of the GNR). The results in the Table represent the stability of the GNRs in each solvent. The PEM, CTAB, and Si-GNRs were only stable in alcohols or polar solvents, albeit the PEM and Si-GNRs were stable for a longer period of time. Purified CTAB-GNRs were generally stable for approximately 24 h or less due to the dissolution of the CTAB into solution and aggregation of GNRs. To maintain the stability of CTAB-GNRs, excess CTAB must be present in the solution. This represents a significant disadvantage for CTAB-GNRs when considering composite materials and solvent exchange. PEG-GNRs were stable in each solution, which suggests they are compatible with both polar and nonpolar solvents.

Table. Stability of GNRs with different functional groups (CTAB, PEM, PEG-SH, and Si GNRS). Sources in superscripts.

Solvent	RI[21–24]	Relative polarity (to water)[22]	CTAB	PEM	PEG	Si
Water	1.331[21]	1.000	X	X	X	X
2-Propanol	1.380[22]	0.546	X	X	X	X
Dimethylformamide	1.430[23]	0.386	X	X	X	X
Ethanol	1.359[23]	0.654	X	X	X	X
Toluene	1.490[23]	0.099	O	O	X	O
Chloroform	1.440[23]	0.259	O	O	X	O
Acetone	1.356[24]	0.355	O	O	X	O
Tetrahydrofuran	1.407[a]	0.207	O	O	X	O

[a]Sigma-Aldrich
Note: X = stability; O = poor/no stability.

In addition to LSPR being sensitive to the morphology of GNRs, it is also sensitive to the dielectric or RI of the surrounding solution. Higher RIs will result in a linear red shift of λ_{LSPR}. This sensitivity can be measured and applied to sensing-based applications. A linear fit of the $\Delta\lambda_{LSPR}$ versus RIU (corresponding to the Table) is illustrated in Fig. 5; PEG-GNRs (Fig. 5A, lower fit) and Si-GNRs (Fig. 5A, upper fit). A good fit is observed for GNRs functionalized with PEG-SH and corresponds to a sensitivity of 130 nm/RIU (~$7X10^{-3}$ RIU/nm). Similarly, a good fit is observed for GNRs capped with Si with a sensitivity of 96 nm/RIU (~$1X10^{-2}$ RIU/nm). The reduced sensitivity of the Si-GNRs could result in part from a reduced interaction of the surface plasmon with the bulk solution due to the thickness of the Si layer. Interestingly, for the PEM-GNRs a linear trend is observed for PSS (negatively charged) layers but not for the PAH (positively charged) (Fig. 5B). In addition, a larger error is observed in the prediction of λ_{LSPR} of PEM layers when compared with that of the Si and PEG layers. This may arise from the solvent quality of each solution, which impacts the swelling of PEM layers and can lead to different net thicknesses of the PEM and ultimately a different effective RI.

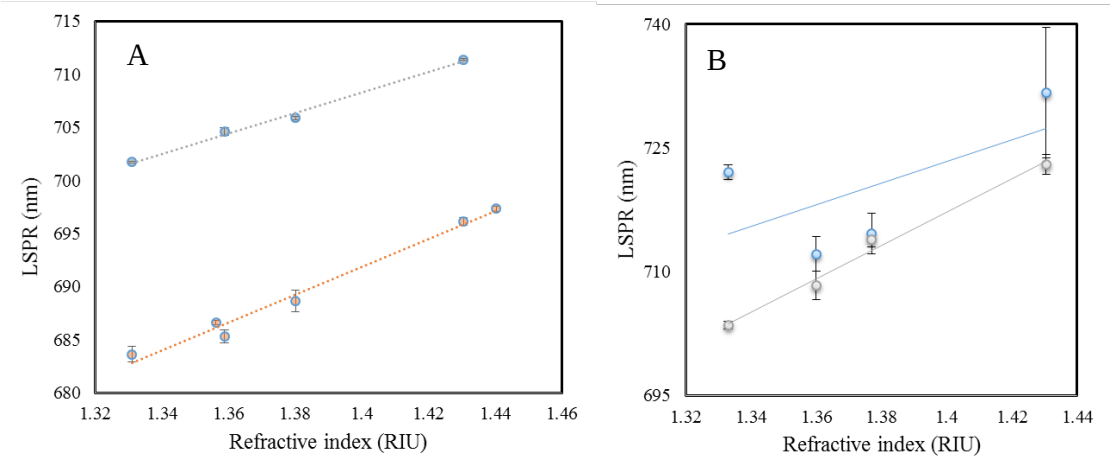

Fig. 5 A) RIU vs. $\Delta\lambda_{LSPR}$ for PEG-functionalized GNRs (orange) and Si-GNRs (grey), respectively, with a linear fit y = 130.7x + 508.8, R_2 = 0.98, and y = 96.0x + 573.9l, R_2 = 0.99. B) RIU vs. $\Delta\lambda_{LSPR}$ for PEM layers (PSS, [–] charge [grey] and PAH [+] charge [blue]).

3.2 Self-Assembly of GNRs

Assembly on TEM grids was accomplished by different deposition methods: fast evaporation (Fig. 6A), slow evaporation (Fig. 6B),[9] and the Langmuir-Schaefer technique (Fig. 6C).[24] For fast evaporation, GNRs functionalized with PVSA were used. The slow evaporation technique was used to deposit CTAB-GNRs. The Langmuir-Schaefer technique was used to deposit the PEG-GNRs due to their ability to successfully disperse in organic solvents, which allowed for their self-assembly at the organic-water interface. Deposition of purified GNRs in acetone with fast evaporation often resulted in high agglomerations (Fig. 6, left) and may result from aggregation induced by the solvent. Deposition from water with slow evaporation resulted in highly dispersed GNRs with some head-to-tail assembly, as depicted in Fig. 6 (center). Good assembly was obtained by the Langmuir-Schaefer method, though GNRs required a functionalization prior to deposition (Fig. 6, right). The Langmuir-Schaefer method is described in literature[24] and in Section 2.6 of this report.

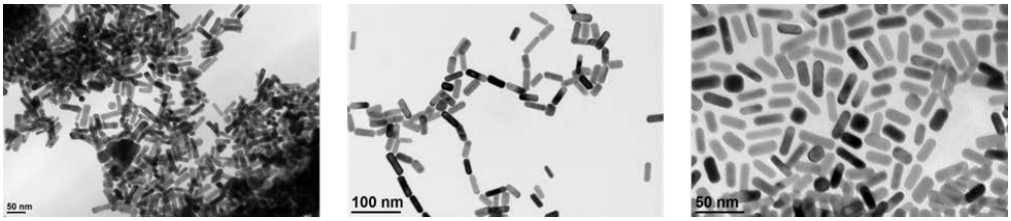

Fig. 6 TEM images of different deposition methods: (left) fast evaporation with an organic solvent, (center) deposition from water with slow evaporation, and (right) the Langmuir-Schaefer technique

3.3 Stability of Dehydrated PEG-GNRs

For many applications, a dehydrated form of GNRs may be preferable to GNRs dispersed in liquid. Unfortunately, CTAB-GNRs that are dried and redispersed in a solvent cannot be regenerated due to aggregation of GNRs and crystallization of residual CTAB. To investigate the regeneration capability of PEG-GNRs, they were dispersed in acetone and dried. Following a 2-day incubation period at ambient conditions, the GNRs were redispersed in water (Fig. 7). A slight blue shift in the LSPR spectra is observed for the rehydrated GNRs (~4 nm) indicating slight aggregation or a reduction of aspect ratio. It has been shown that the shape of GNRs can revert back to a spherical geometry with time or excess processing (heating, solvent exchange, etc.). Additionally, comparing the ratio between the longitudinal (~700 nm) and transverse (~550 nm) resonances for both the control (~1.77) and the regenerated (~1.53) species suggests that there is loss in the geometry (i.e., more of spherical species). Although some loss is observed (~7.8%), the integrity of the GNRs is maintained.

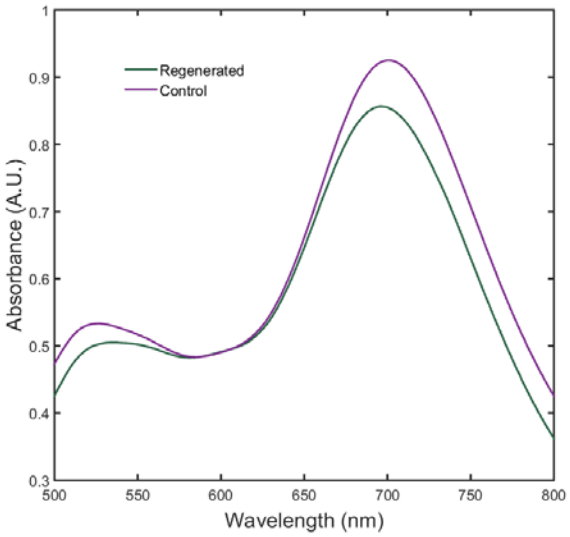

Fig. 7 Effect of drying solution into a powder then redispersing in water on λ_{LSPR}

4. Summary and Conclusions

The stability of GNRs in various solvents was evaluated to assess the impact of 3 surface functionalization strategies. The compatibilization of GNRs with nonaqueous solvents opens the window for integrating GNRs into solvent-borne composite applications. In particular, the GNRs were functionalized by surface moeities to improve stability and resist aggregation in both solvated (aqueous/organic) and dry conditions. The specific surface modifications installed included PEMs, PEG, and Si as the outer layer of the GNRs. Results suggest that

GNRs functionalized with PEG-SH are stable in both hydrophillic and hydrophobic solvents and exhibited the most versatility of the surface modifications studied. Importantly, all the functionalized GNRs examined in this study exhibited greater temporal stability in water than the CTAB-GNRs. The λ_{LSPR} for both the PEG- and Si-GNRs revealed a linear shift with increasing refractive index, whereas the PEM layers demonstrated greater inconsistencies in the λ_{LSPR} prediction with RI. This suggests the PEM layers are more susceptable to interactions with the respective solvent. In addition, an approximately 26% decrease in senstivity was observed for GNRs functionalized with Si compared with the PEG layers. Self-assembly was achieved by depositing layers of GNRs onto TEM grids by the Langmuir-Shaeffer technique, which is important, as it avoids aggregation and may be useful for deposition of GNRs on various materials. Finally, investigations into the stability of dried PEG-GNRs revealed excellent regeneration capabilities with limited material loss (~7.8%). Untimately, these studies demonstrate the compatibility of functionalized GNRs in various solvents for use in functional composite applications.

5. References

1. Vigderman L, Khanal BP, Zubarev ER. Functional gold nanorods: synthesis, self-assembly, and sensing applications. Adv Mater. 2012;24:4811–4841.

2. Kah J, Yeo E, He S, Engudar G. Gold nanorods in photomedicine. In: Hamblin M, Avci P, editors. Applications of nanoscience in photomedicine. Waltham (MA): Woodhead Publishing; 2015. p. 221–240.

3. Huang X, El-Sayed IH, Qian W, El-Sayed MA. Cancer cell imaging and photothermal therapy in the near-infrared region by using gold nanorods. J Am Chem Soc. 2006;128(6):2115–2120.

4. Rey A, Billardon G, Lörtscher E, Moth-Poulsen K, Stuhr-Hansen N, Wolf H, Bjørnholm T, Stemmer A, Riel H. Deterministic assembly of linear gold nanorod. Nanoscale. 2013;5(18):8680–8688.

5. Mubeen S, Lee J, Lee W, Singh N, Stucky GD, Moskovits M. On the plasmonic photovoltaic. ACS Nano. 2014;8(6):6066–6073.

6. Wadamsa RC, Yen C, Butcher DP, Koerner H, Durstock MF, Fabris L, Tabor CE. Gold nanorod enhanced organic photovoltaics: the importance of morphology effects. Org Elec. 2014;15;1448–1457.

7. Lee K, El-Sayed MA. Gold and silver nanoparticles in sensing and imaging: sensitivity of plasmon response to size, shape, and metal composition. J Phys Chem B. 2006;110:19220–19225.

8. Scaletti F, Kim CS, Messori L, Rotello VM. Rapid purification of gold nanorods for biomedical applications. MethodsX. 2014;1:118–123.

9. Alkinlany AM, Thompson LB, Murphy CJ. Polyelectrolyte coating provides a facile route to suspend gold nanorods in polar organic solvents and hydrophobic polymers. Appl Mater Inter. 2010;2(12):3417–3421.

10. Ye X, Jin L, Caglayan H, Chen J, Xing G, Zheng C, Murray CB. Improved size-tunable synthesis of monodisperse gold nanorods through the use of aromatic additives. ACS Nano. 2012;6(3):2804–2817.

11. Nikoobakht B, El-Sayed MA. Preparation and growth mechanism of gold nanorods using seed-mediated growth method. Chemistry of Materials. 2003;15(10):1957–1962.

12. Zubarev LV. High-yield synthesis of gold nanorods with longitudinal SPR peak greater than 1200 nm using hydroquinone as a reducing agent. Chemistry of Materials. 2013;25(8):1450–1457.

13. Scarabelli L, Grzelczak M, Liz-Marzán LM. Tuning gold nanorod synthesis through prereduction with salicylic acid. Chemistry of Materials. 2013;25(21):4232–4238.

14. Pierrat S, Zins I, Breivogel A, Sönnichsen C. Self-assembly of small gold colloids with functionalized gold nanorods. Nano Letters. 2007;7(2):259–263.

15. Abadeer N, Brennan M, Wilson W, Murphy C. Distance and plasmon wavelength dependent fluorescence of molecules bound to silica-coated gold nanorods. ACS Nano. 2014;8(8):8392–8406.

16. Pastoriza-Santos I, Pérez-Juste J, Liz-Marzán LM. Silica-coating and hydrophobation of CTAB-stabilized gold nanorods. Chemistry of Materials. 2006;10(18):2465–2467.

17. Li X, Qian J, He S. Impact of the self-assembly of multilayer polyelectrolyte functionalized gold nanorods and its application to biosensing. Nanotechnology. 2008;19(35):355501.

18. Kinnear C, Dietsch H, Clift MJ, Endes C, Rothen-Rutishauser B, Petri-Fink A. Gold nanorods: controlling their surface chemistry and complete detoxification by a two-step place exchange. Angew Chem Int Ed. 2013;52(7):1934–1938.

19. Huang J. Jackson K, Murphy CJ. Polyelectrolyte wrapping layers control rates of photothermal molecular release from gold nanorods. Nano Letters. 2012;12(6):2982–2987.

20. Kegel LL, Menegazzo N, Booksh KS. Adsorbate–metal bond effect on empirical determination of surface plasmon penetration depth. Anal Chem. 2013;85(10):4875–4883.

21. Hale GM, Querry MR. Optical constants of water in the 200-nm to 200-µm wavelength region. Appl Opt. 1973;12:555–563.

22. Moutzouris K, Papamichael M, Betsis SC, Stavrakas I, Hloupis G, Triantis D. Refractive, dispersive and thermo-optic properties of twelve organic solvents in the visible and near-infrared. Applied Physics B. 2013;116:617–622.

23. Kedenburg, S, Vieweg M, Gissibl T, Giessen H. Linear refractive index and absorption measurements of nonlinear optical liquids in the visible and near-infrared spectral region. Optical Materials Express. 2012;2:1588–1611.

24. Scarabelli L, Coronado-Puchau M, Giner-Casares JJ, Langer J, Liz-Marzán LM. Monodisperse gold nanotriangles: size control, large-scale self-assembly, and performance in surface-enhanced raman scattering. ACS Nano. 2014;8(6):5833–5842.

List of Symbols, Abbreviations, and Acronyms

$AgNO_3$	silver nitrate
λ_{LSPR}	wavelength
ARL	US Army Research Laboratory
Au	gold
CTAB	cetyl trimethyl ammonium bromide
EM	electromagnetic
GNP	gold nanoparticle
GNR	gold nanorod
HQ	hydroquinone
LSPR	localized surface plasmon resonance
NaOH	sodium hydroxide
Na-Sal	sodium salicylate
ORISE	Oak Ridge Institute for Science and Education
PAH	poly(allyamine hydrochloride)
PEG	polyethylene glycol
PEG-SH	polyethylene glycol thiol
PEM	polyelectrolyte monolayer
PSS	polystyrene sulfonate
PVSA	poly(vinylsulfonic acid)
RI	refractive index
RIU	refractive index unit
Si	silicon/silica
SPR	surface plasmon resonance
TEM	transmission electron microscope/microscopy
UV-vis	ultraviolet-visible

1 (PDF) DEFENSE TECHNICAL INFORMATION CTR DTIC OCA

2 (PDF) DIRECTOR US ARMY RESEARCH LAB RDRL CIO LL IMAL HRA MAIL & RECORDS MGMT

1 (PDF) GOVT PRINTG OFC A MALHOTRA

1 (PDF) DIR USARL RDRL WMM A M GRIEP

INTENTIONALLY LEFT BLANK.